

RAPID COMMUNICATION | OCTOBER 11 2023

Signature of functional enzyme dynamics in quasielastic neutron scattering spectra: The case of phosphoglycerate kinase

Abir N. Hassani ; Luman Haris ; Markus Appel ; Tilo Seydel ; Andreas M. Stadler ; Gerald R. Kneller  



J. Chem. Phys. 159, 141102 (2023)

<https://doi.org/10.1063/5.0166124>



CrossMark

Articles You May Be Interested In

A functional integral formalism for quantum spin systems

J. Math. Phys. (July 2008)

Modes selection in polymer mixtures undergoing phase separation by photochemical reactions

Chaos (June 1999)

Spreading of a surfactant monolayer on a thin liquid film: Onset and evolution of digitated structures

Chaos (March 1999)

500 kHz or 8.5 GHz?
And all the ranges in between.

Lock-in Amplifiers for your periodic signal measurements



Find out more



Signature of functional enzyme dynamics in quasielastic neutron scattering spectra: The case of phosphoglycerate kinase

Cite as: *J. Chem. Phys.* **159**, 141102 (2023); doi: [10.1063/5.0166124](https://doi.org/10.1063/5.0166124)

Submitted: 3 July 2023 • Accepted: 25 September 2023 •

Published Online: 11 October 2023



View Online



Export Citation



CrossMark

Abir N. Hassani,^{1,2}  Luman Haris,^{2,3}  Markus Appel,⁴  Tilo Seydel,⁴  Andreas M. Stadler,^{2,3,a)} 
and Gerald R. Kneller^{1,5,b)} 

AFFILIATIONS

¹Centre de Biophysique Moléculaire, CNRS and Université d'Orléans, Rue Charles Sadron, 45071 Orléans, France

²Jülich Centre for Neutron Science (JCNS-1) and Institute of Biological Information Processing (IBI-8), Forschungszentrum Jülich GmbH, 52425 Jülich, Germany

³Institute of Physical Chemistry, RWTH Aachen University, Landoltweg 2, 52056 Aachen, Germany

⁴Institut Laue Langevin, 71 Avenue des Martyrs, 38042 Grenoble Cedex 9, France

⁵Laboratoire des biomolécules, Département de chimie, Ecole Normale Supérieure, 75005 Paris, France

^{a)}E-mail: a.stadler@fz-juelich.de

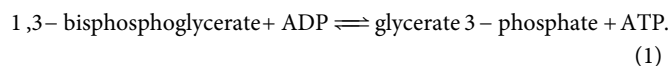
^{b)}Author to whom correspondence should be addressed: gerald.kneller@cnrs.fr

ABSTRACT

We present an analysis of high-resolution quasi-elastic neutron scattering spectra of phosphoglycerate kinase which elucidates the influence of the enzymatic activity on the dynamics of the protein. We show that in the active state the inter-domain motions are amplified and the intra-domain asymptotic power-law relaxation $\propto t^{-\alpha}$ is accelerated, with a reduced coefficient α . Employing an energy landscape picture of protein dynamics, this observation can be translated into a widening of the distribution of energy barriers separating conformational substates of the protein.

Published under an exclusive license by AIP Publishing. <https://doi.org/10.1063/5.0166124>

Understanding the functional dynamics of enzymes is a fundamental issue in molecular biophysics, biology, and biochemistry. Phosphoglycerate kinase (PGK) is one example for which the dynamics-function relationship has been intensively studied with various methods, including structural nuclear magnetic resonance (NMR), x-ray crystallography, quasielastic neutron scattering (QENS), neutron spin echo (NSE) spectroscopy, and molecular dynamics (MD) simulation.^{1–10} PGK is a monomeric enzyme which is fundamental for the metabolism of all living organisms. By converting 1,3-bisphosphoglycerate to 3-phosphoglycerate it catalyzes one of the two ATP-producing reactions of the glycolytic pathway and it participates also in gluconeogenesis by catalyzing the opposite reaction to produce 1,3-bisphosphoglycerate and adenosine diphosphate phosphate (ADP),¹¹



Yeast PGK has a weight of about 45 kDa and is composed of two domains which are connected by a well conserved hinge region where the catalytic reactions take place. Several of the studies cited above have been performed with the particular goal to better understand the role of the inter-domain motions for the function of the enzyme.^{4,6,7,9} A powerful space and time-resolved method for this purpose is neutron spin echo (NSE) spectroscopy, which has been used in Ref. 7 in combination with small-angle neutron scattering (SANS) and normal mode analysis and in Ref. 9 in combination with MD simulation. Standard NSE probes the slow motions and global diffusion of proteins on a 0.1–100 ns time scale and on a nm length scale. The results of the NSE studies suggest that the hinge-bending motions of the two domains in PGK enable its enzymatic activity and that the presence of the substrates rigidifies the molecular and accelerates its internal dynamics.

The present article aims at extending and consolidating the abovementioned work with an analysis of QENS data from the high-resolution spectrometer IN16B at the Institut Laue-Langevin

in Grenoble. The instrument probes the ns time scale if operated in BATS mode (backscattering and time of flight spectroscopy)¹² and closes the gap between QENS experiments with standard time-of-flight spectrometers and NSE spectroscopy.

The QENS experiments on PGK were performed at 283 K in presence and absence of the substrates (13 mM MgATP, 41 mM 3PG, 20 mM MOPS, 50 mM NaCl, 2 mM EDTA, pD 7.4, 99.9% atom D deuteriumoxide) using a PGK concentration of 50 mg/ml. PGK from yeast and all chemicals were obtained commercially from Sigma-Aldrich. These conditions are the same as in Ref. 7 and warrant that PGK in presence of substrates is more than 90% in the ligand-bound state. Prior to data analysis, the solvent-contributions were subtracted. Since about 50% of the atoms in a protein are hydrogen atoms, which have a strongly dominant cross section for incoherent neutron scattering, the dynamic structure factor for QENS from PGK can be written in the form

$$S(\mathbf{q}, \omega) = \frac{1}{2\pi} \int_{-\infty}^{+\infty} dt e^{-i\omega t} F(\mathbf{q}, t), \quad (2)$$

$$F(\mathbf{q}, t) \approx \frac{1}{N} \sum_{j \in \mathbb{H}} \left\langle e^{-i\mathbf{q} \cdot \hat{\mathbf{x}}_j(0)} e^{i\mathbf{q} \cdot \hat{\mathbf{x}}_j(t)} \right\rangle. \quad (3)$$

Here N is the number of hydrogen atoms, $\hat{\mathbf{x}}_j(t)$ is the time-dependent position operator of hydrogen atom j , \mathbf{q} the scattering vector, and the symbol $\langle \dots \rangle$ denotes a quantum ensemble average. The latter leads to the symmetry relations $F^*(\mathbf{q}, t) = F(\mathbf{q}, -t)$ and $F(\mathbf{q}, t) = F(-\mathbf{q}, -t + i\beta\hbar)$.

As in several previous studies,^{13–16} the analysis of the QENS data has been performed in the time domain, employing a stochastic model for the classical intermediate scattering function and assuming that Schofield's semiclassical approximation^{17,18} is valid.

For model building purposes, we assume that there is a representative hydrogen atom “ a ” whose dynamics accounts for both the relaxation dynamics of the individual hydrogen atoms and their motional heterogeneity. Within Schofield's semiclassical approximation we have then

$$F^{(+)}(\mathbf{q}, t) \approx \left\langle e^{-i\mathbf{q} \cdot \hat{\mathbf{x}}_a(0)} e^{i\mathbf{q} \cdot \hat{\mathbf{x}}_a(t)} \right\rangle_{\text{cl}}, \quad (4)$$

where $\langle \dots \rangle_{\text{cl}}$ stands for a classical ensemble average. We assume furthermore that the domains in PGK can be treated as equivalent and that the motions of the scattering atom are uncorrelated with the motions of the domain to which it is attached. Writing $\mathbf{x}_a = \mathbf{R}_a + \mathbf{r}_a$, where \mathbf{R}_a points to the center of the domain and \mathbf{r}_a to the position of the scattering atom with respect to that reference point (see Fig. 1), the orientation-averaged intermediate scattering function of PGK in solution can then be factorized as

$$\bar{F}^{(+)}(q, t) \approx f(q, t)g(q, t) \quad (q \equiv |\mathbf{q}|), \quad (5)$$

where

$$f(q, t) \equiv \overline{\langle a_q^* a_q(t) \rangle_{\text{cl}}} \quad \text{and} \quad g(q, t) \equiv \overline{\langle A_q^* A_q(t) \rangle_{\text{cl}}} \quad (6)$$

are the orientation-averaged autocorrelation functions related to the respective dynamical variables

$$A_q \equiv e^{i\mathbf{q} \cdot \mathbf{R}_a} \quad \text{and} \quad a_q \equiv e^{i\mathbf{q} \cdot \mathbf{r}_a}. \quad (7)$$

Both are to be understood as complex stochastic variables, depending parametrically on the respective position vectors and on \mathbf{q} , whose time evolution is described by appropriate diffusion models to be described in the following. Conceptually our approach can be compared to modeling reaction coordinates describing protein folding,¹⁹ and it has been used so far to model QENS from the internal dynamics of proteins and from water (see Refs. 13–16 cited above). We apply it here in addition to account for inter-domain motions in PGK by a refined model compared to the one we used in our recent study of Myelin Basic Protein (MBP).¹⁴ Defining

$$\xi \equiv \begin{pmatrix} \Re\{A_q - \langle A_q \rangle_{\text{cl}}\} \\ \Im\{A_q - \langle A_q \rangle_{\text{cl}}\} \end{pmatrix}, \quad (8)$$

we consider in particular that the conditional probability, $P(\xi, t | \xi_0, 0)$ for a transition $\xi_0 \rightarrow \xi$ within time t describes an Ornstein–Uhlenbeck (OU) process,²⁰ i.e., diffusion in a harmonic potential (left part of Fig. 2),

$$\partial_t P = \left\{ \eta_\xi \frac{\partial}{\partial \xi} \cdot \{ \xi P \} + D_\xi \frac{\partial}{\partial \xi} \cdot \frac{\partial P}{\partial \xi} \right\}. \quad (9)$$

Here η_ξ is a relaxation constant and D_ξ is a diffusion coefficient which can be related to η_ξ via $D_\xi = \eta_\xi k_B T / K_\xi = \eta_\xi \langle |\xi|^2 \rangle_{\text{cl}}$, with K_ξ being the force constant of the harmonic potential. We assume in particular that $\langle A_q \rangle \rightarrow 0+$, without vanishing identically, such that ξ_1 and ξ_2 can be formally considered as independent dynamical variables. The essential point is that the autocorrelation function of ξ decays exponentially,

$$\langle \xi^T(0) \cdot \xi(t) \rangle_{\text{cl}} = \langle |\xi(0)|^2 \rangle_{\text{cl}} e^{-\eta_\xi t}, \quad \eta_\xi \equiv \eta_\xi(\mathbf{q}). \quad (10)$$

Since $\langle A_q \rangle \approx 0$ for a freely diffusing particle it follows that $\langle |\xi(0)|^2 \rangle_{\text{cl}} \approx 1$, and we write therefore

$$g(q, t) = e^{-D(q)q^2|t|}, \quad (11)$$

assuming that the relaxation coefficient $\eta_\xi(\mathbf{q})$ does not depend on the direction of \mathbf{q} . The parameter $D(q)$ is here a q -dependent diffusion coefficient. For small q -values it follows from the cumulant expansion of the intermediate scattering function that

$$g(q, t) \stackrel{q \rightarrow 0}{\approx} e^{-\frac{q^2}{6} \langle (\mathbf{R}_a(t) - \mathbf{R}_a(0))^2 \rangle_{\text{cl}}} \stackrel{t \rightarrow \infty}{\approx} e^{-D_0 q^2 t}. \quad (12)$$

where D_0 is the diffusion coefficient for a whole domain and thus for the whole PGK molecule. For finite q -values $g(q, t)$ describes the diffusion of whole PGK molecules which is modulated by inter-domain motions.

For the intra-domain dynamics we use the same model as for the internal protein dynamics in Refs. 13 and 14 and in the light of the preceding discussions the dynamics of the vector variable

$$\chi \equiv \begin{pmatrix} \Re\{a_q - \langle a_q \rangle_{\text{cl}}\} \\ \Im\{a_q - \langle a_q \rangle_{\text{cl}}\} \end{pmatrix}, \quad (13)$$

is described by a fractional Ornstein Uhlenbeck process,^{21,22}

$$\partial_t p = {}_0\partial_t^{1-\alpha} \left\{ \eta_\chi^{(\alpha)} \frac{\partial}{\partial \chi} \cdot \{ \chi p \} + D_\chi^{(\alpha)} \frac{\partial}{\partial \chi} \cdot \frac{\partial p}{\partial \chi} \right\}. \quad (14)$$

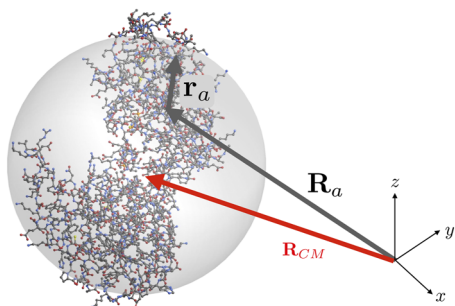


FIG. 1. The PGK molecule (PDB code 3PGK) together with a sphere of radius $R_H = 30.5$ Å which is used for the Stokes–Einstein relation (18) and the definitions of R_α and r_α . The red arrow points to the center-of-mass.

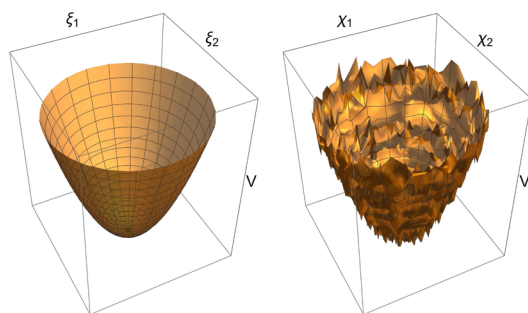


FIG. 2. Smooth harmonic potential (left) and its rough counterpart (right) steering the diffusion of ξ and χ , respectively.

Here $0 < \alpha < 1$ and ${}_0D_t^{1-\alpha}$ denotes a fractional derivative of order $1 - \alpha$ with respect to t ,²³ $\eta_\chi^{(\alpha)}$ is a fractional relaxation constant, and $D_\chi^{(\alpha)}$ the corresponding fractional diffusion coefficient. The autocorrelation function of χ evolves according to

$$\langle \chi^T(0) \cdot \chi(t) \rangle_{cl} = \langle |\chi|^2 \rangle_{cl} E_\alpha(-\eta_\alpha t^\alpha), \quad \eta_\alpha \equiv \eta_\alpha(\mathbf{q}), \quad (15)$$

where $E_\alpha(-\eta_\alpha t^\alpha)$ is a stretched Mittag-Leffler (ML) function,^{23,24} which interpolates between a stretched exponential at short times and an inverse power law at long times and converges to a simple exponential (Debye relaxation) for $\alpha \rightarrow 1$. Noting that $\overline{\langle |\chi|^2 \rangle}_{cl} = 1 - EISF(q)$, where $EISF(q) \equiv \overline{\langle |a_q| \rangle}_{cl}^2$ is the elastic intensity of an isotropic system, we arrive at

$$f(q, t) \equiv EISF(q) + (1 - EISF(q)) E_\alpha(-(|t|/\tau)^\alpha). \quad (16)$$

Here $EISF(q)$, $\tau \equiv \tau(q)$, and $\alpha \equiv \alpha(q)$ are considered as q -dependent fit parameters. The fractional Ornstein–Uhlenbeck process can be visualized as diffusion process in a “rough” two-dimensional harmonic potential (right part Fig. 2), which is characterized by a wide distribution of energy barriers separating various minima or “conformational substates.”²⁵ In the framework of the Generalized Langevin Equation²⁶ the correlation function (15) is characterized by a memory function with an algebraic long time tail $\propto t^{\alpha-2}/\Gamma(\alpha-1)$ whose amplitude vanishes for $\alpha \rightarrow 1$. We note here

that the parameter α entirely determines the distribution function for the dimensionless barrier, $\epsilon = \Delta E/k_B T$,

$$P_{ML}(\epsilon) = \frac{2\epsilon \sin(\pi\alpha)}{\pi(e^{-\alpha\epsilon^2} + e^{\alpha\epsilon^2} + 2\cos(\pi\alpha))}. \quad (17)$$

For $\alpha \rightarrow 1$ the barrier distribution, $P_{ML}(\epsilon)$, is entirely concentrated on $\epsilon = 0$.

We start the discussion of the results with the right panel of Fig. 3, which shows a fit of the resolution-deconvolved intermediate scattering function, $\overline{F}^{(+)}(q, t) \approx f(q, t)g(q, t)$, with four parameters, $\tau(q)$, $\alpha(q)$, $EISF(q)$, and $D(q)$ for the minimum and maximum q -values in absence and presence of substrates. The data reduction has been performed with the MANTID package²⁷ and the code for the data analysis has been developed with Wolfram Mathematica.²⁸ Figure 4 displays the parameters τ (left panel) and α (right panel) as a function of q in presence and absence of the substrates (blue and yellow triangles, respectively). A clear impact of the presence of substrates on the intra-domain dynamics can be seen: Both τ and α are systematically reduced in presence of the substrates, which indicates that the internal molecular dynamics is accelerated by the enzymatic activity of the molecule and that the relaxation dynamics of the domains becomes less exponential. We note that τ and α in presence and absence of the substrates follow globally the same evolution with q . The time scale parameter τ becomes generally smaller with increasing q , which simply indicates that localized motions are faster than collective motions implying a large number of atoms. The form parameter, α , increases instead with q to values close to 1, indicating increasingly exponential relaxation for more localized motions. We attribute this behavior to the fact that less relaxation modes contribute to localized motions than to large amplitude motions which are probed at small values of q .

Figure 5 presents the fitted EISFs together with the integrated measured QENS intensity over the width of the resolution function, which can be considered as measured counterpart. The difference

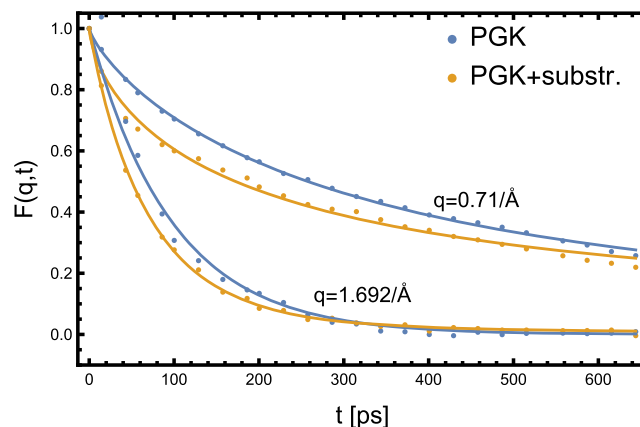


FIG. 3. Resolution-deconvolved $F(q, t)$ of PGK in deuterated solution without and in presence of substrates (blue and yellow dots, respectively) and the corresponding fits (blue and yellow line, respectively).

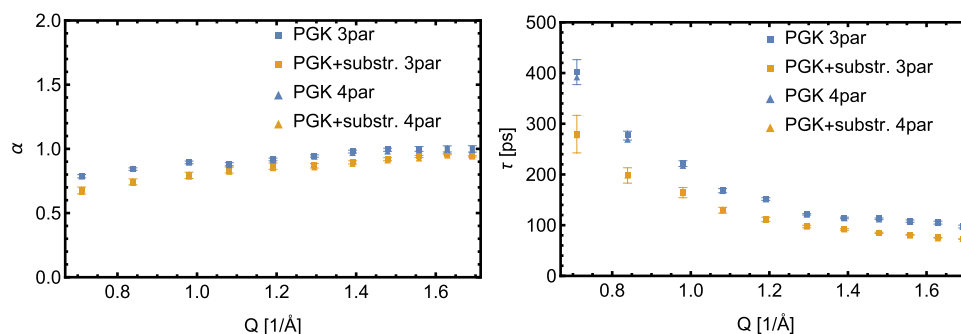


FIG. 4. The model parameters τ and α for PGK. Triangles indicate four-parameter fits (no error bars given) and squares three-parameter fits (with error bars). More explanations are given in the text.

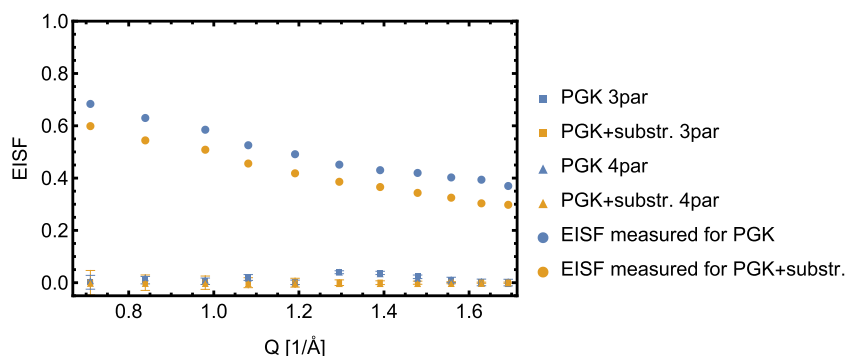


FIG. 5. The EISF parameter for PGK in absence and presence of substrates.

between the two can be attributed to unavoidable spurious contributions from quasielastic scattering, which are due to finite instrumental resolution. They are here estimated on the basis of the underlying model for the relaxation function, $\phi(q, t) \equiv E_\alpha(-|t/\tau|^\alpha)$, and the measured elastic intensity. The details can be found in Ref. 29. We find that the fitted EISF is globally close to zero in the presence and absence of the ligand, except at $q = 1.3 \text{ \AA}^{-1}$ where the EISF of PGK in absence of substrates ligand is slightly larger than the EISF in their presence. Correlating this observation with the decrease of α in presence of the substrates shows that the domains are slightly stiffened, which confirms again the findings in Ref. 7 which were obtained by NSE spectroscopy.

For comparison we show also fits with a reduced model where $D(q) \equiv 0$ (blue and yellow squares, respectively). It can be clearly seen that the results are very similar, the difference being the error bars, which are much larger for the fit of all four parameters and which are not shown here. This observation is in line with the findings in Ref. 14 for the intrinsically disordered Myelin Basic Protein (MBP) and we present the three-parameter fits to show that the fits of τ , α and EISF are stable.

The impact of the enzymatic dynamics on the intra-domain energy landscape can be visualized by comparing the energy barrier profiles, $P_{ML}(\epsilon)$, describing its “roughness,”^{13,14} which are displayed in the left panel of Fig. 6. Important differences between the two profiles are again observed for q -values corresponding to opening

amplitudes of the hinge region and indicate a wider distribution of energy barriers in presence of the substrates. This corresponds to the decrease of the alpha parameter described above, indicating a stiffening of PGK in its active mode.

The q -dependent diffusion coefficient is displayed in the right panel of Fig. 6. One observes that $D(q)$ displays a pronounced modulation with respect to its values at small and large q -values. The latter are close to the estimation for the diffusion coefficient of a whole PGK molecule obtained from the Stokes–Einstein law,

$$D_0 = \frac{k_B T}{6\pi\eta R_H} \approx 5.1 \times 10^{-3} \text{ \AA}^2/\text{ps}. \quad (18)$$

For this estimation we used an effective hydrodynamic radius of $R_H = 30.5 \text{ \AA}$ calculated from the PDB structure 3PGK, including the diameter of a water molecule (see Fig. 1). The maximum of $D(q)$ at about $q_{\max} \approx 1.2 \text{ \AA}^{-1}$ corresponds to $2\pi/q_{\max} \approx 5 \text{ \AA}$ in real space, which can be associated with breathing motions of the hinge-region in PGK caused by its enzymatic activity and which have also been observed by combining NSE spectroscopy, normal mode analysis, and hydrodynamic molecular modelling.⁷ The fact that $D(q) \approx D_0$ for smaller q -values is in line with the requirement that $g(q, t)$ must here describe diffusion of whole PGK molecules and $D(q) \approx D_0$ at

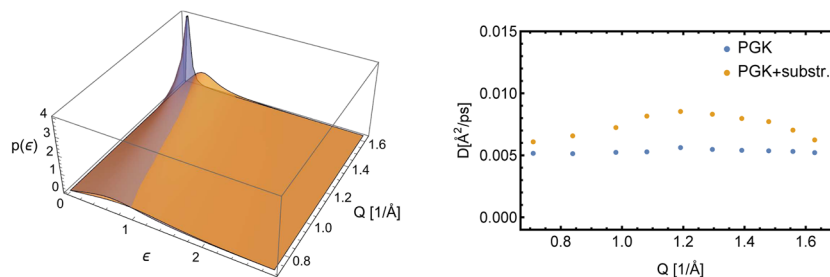


FIG. 6. Left panel: Energy barrier spectrum in absence (blue) and presence (yellow) of substrates. Right panel: The fitted diffusion coefficient $D(q)$.

higher q -values reflects that more localized motions do not affect the global diffusive dynamics of PGK.

To resume, we can say that our QENS study gives a consistent picture of the functional dynamics of PGK which confirms and completes an earlier study by NSE spectroscopy. It shows in particular that the “minimalistic” model used in this work suffices to extract the essential information in the QENS data through a physical interpretation of q -dependent model parameters. In this context the strongly non-exponential relaxation dynamics in proteins is a key element which must be accounted for to fully exploit the rich information content in the QENS data. We finally remark that the concept can be easily extended to describe also coherent scattering. In this case one simply considers collective dynamical variables of the form $\alpha_q \equiv \sum_j \exp(iq \cdot \mathbf{x}_j)/\sqrt{N}$.

We gratefully acknowledge beam time allocation on the IN16B neutron spectrometer at the Institut Laue-Langevin, Grenoble, France. A.N.H. acknowledges financial support from the Région Centre - Val de Loire and the Jülich Centre for Neutron Science.

AUTHOR DECLARATIONS

Conflict of Interest

The authors have no conflicts to disclose.

Author Contributions

Abir N. Hassani: Formal analysis (lead); Investigation (equal); Methodology (supporting); Software (equal); Visualization (lead); Writing – original draft (supporting). **Luman Haris:** Investigation (supporting). **Markus Appel:** Investigation (equal); Resources (equal). **Tilo Seydel:** Investigation (equal); Resources (equal). **Andreas M. Stadler:** Conceptualization (equal); Investigation (lead); Resources (equal); Writing – original draft (supporting). **Gerald R. Kneller:** Conceptualization (lead); Formal analysis (supporting); Investigation (equal); Methodology (lead); Software (equal); Supervision (lead); Writing – original draft (lead).

DATA AVAILABILITY

The data that support the findings of this study are openly available at <http://doi.org/10.5291/ILL-DATA.8-04-916> and the analysis software under <https://doi.org/10.5281/zenodo.8396244>.

REFERENCES

- P. Tanswell, E. W. Westhead, and R. J. P. Williams, *Eur. J. Biochem.* **63**, 249 (1976).
- R. D. Banks *et al.*, *Nature* **279**, 773 (1979).
- M. A. Sinev, O. I. Razgulyaev, M. Vas, A. A. Timchenko, and O. B. Ptitsyn, *Eur. J. Biochem.* **180**, 61 (1989).
- B. E. Bernstein, P. A. M. Michels, and W. G. J. Hol, *Nature* **385**, 275 (1997).
- E. Balog *et al.*, *Phys. Rev. Lett.* **93**, 028103 (2004).
- Z. Palmal *et al.*, *Proteins: Struct., Funct., Bioinf.* **77**, 319 (2009).
- R. Inoue *et al.*, *Biophys. J.* **99**, 2309 (2010).
- E. Balog, D. Perahia, J. C. Smith, and F. Merzel, *J. Phys. Chem. B* **115**, 6811 (2011).
- N. Smolin, R. Biehl, G. R. Kneller, D. Richter, and J. C. Smith, *Biophys. J.* **102**, 1108 (2012).
- X. Hu *et al.*, *Nat. Phys.* **12**, 171 (2016).
- P. D. Boyer, *The Enzymes. 8: Group Transfer. Part A: Nucleotidyl Transfer, Nucleosidyl Transfer, Acyl Transfer, Phosphoryl Transfer*, 3rd ed. (Academic Press, New York, 1973).
- M. Appel, B. Frick, and A. Magerl, *Physica B* **562**, 6 (2019).
- M. Saouessi, J. Peters, and G. R. Kneller, *J. Chem. Phys.* **150**, 161104 (2019).
- A. N. Hassani *et al.*, *J. Chem. Phys.* **156**, 025102 (2022).
- M. H. Petersen *et al.*, *J. Phys. Chem. C* **125**, 15085 (2021).
- M. H. Petersen, M. T. F. Telling, G. Kneller, and H. N. Bordallo, *EPJ Web Conf.* **272**, 01012 (2022).
- G. R. Kneller, *Proc. Natl. Acad. Sci. U. S. A.* **115**, 9450 (2018).
- P. Schofield, *Phys. Rev. Lett.* **4**, 239 (1960).
- J. N. Onuchic, Z. Luthey-Schulten, and P. G. Wolynes, *Annu. Rev. Phys. Chem.* **48**, 545 (1997).
- G. Uhlenbeck and L. Ornstein, *Phys. Rev.* **36**, 823 (1930).
- R. Metzler, J. H. Jeon, A. G. Cherstvy, and E. Barkai, *Phys. Chem. Chem. Phys.* **16**, 24128 (2014).
- R. Metzler and J. Klafter, *Phys. Rep.* **339**, 1 (2000).
- Mittag-Leffler Functions, Related Topics and Applications*, Springer Monographs in Mathematics, edited by R. Gorenflo, A. A. Kilbas, F. Mainardi, and S. V. Rogosin (Springer, Heidelberg, 2014).
- W. G. Glöckle and T. F. Nonnenmacher, *Biophys. J.* **68**, 46 (1995).
- H. Frauenfelder, S. G. Sligar, and P. G. Wolynes, *Science* **254**, 1598 (1991).
- R. Zwanzig, *Nonequilibrium Statistical Mechanics* (Oxford University Press, Oxford; New York, 2001).
- O. Arnold, *Nucl. Instrum. Methods Phys. Res., Sect. A* **764**, 156 (2014).
- Wolfram Research, Inc., Mathematica, Version 13.2, Champaign, IL, 2021.
- A. N. Hassani, A. M. Stadler, and G. R. Kneller, *J. Chem. Phys.* **157**, 134103 (2022).